Study on Flow Field in a Bifurcation Lung Airway Model

J. Y. Lin*, L. C. Lee, M. L. Lee, C. Y. Shen, and R. J. Shih

National Center for High Performance Computing, Hsinchu, Taiwan, R.O.C.

c00jyl00@nchc.org.tw

Abstract: A computational fluid dynamics (CFD) modelling approach is used to study the unsteady respiratory airflow dynamics within a human lung. The three-dimensional symmetric bifurcation model of the central airway based on the morphological data given by Weibel [1] was used in the present study to simulate the oscillatory flow in the respiratory system. Comparing the flow fields in the decelerating phase and accelerating phase of the inspiratory flow, we can observe some subtle differences. The secondary motions were generated due to the complex geometry. With the CFD modelling, it is possible to develop an insight into airflow patterns and obtain valuable information, which will help physicians to avoid inappropriate clinical trials and unnecessary effort.

Introduction

The respiratory diseases such as asthma, emphysema and bronchitis are connected with the air pollution in the urban environment and the number of these diseases increases every year. The therapy of respiratory diseases mostly uses pharmaceuticals in the form of aerosol delivered into the lungs. The efficiency and efficacy of the therapy depend on the particle size of the drugs and their transport and deposition in the lungs. Very little information on the pattern of the particle deposition or the effectiveness of the aerosol treatment is available, and thus attracts many clinical respiratory researches to step into this area.

The respiratory system can be characterized by a network of dichotomous bronchia [1] and its airflow mechanisms can be studied through physical modelling of the respiratory airflow network. However, knowledge of the airflow mechanism within the airway is the first step toward understanding of the movement of the particles and their deposition in the respiratory airflow network.

Investigating inspiratory and expiratory airway flows undoubtedly can be accomplished by using scaled-up laboratory models. Such experiments are, however, expensive and time consuming. Owing to rapid advances in computer technology and improving numerical techniques, computational fluid dynamics (CFD) offers an alternative to study the airflow employing a physical realistic model. An additional advantage is that numerical simulation allows investigation of various modelling conditions, which may not be possible in a laboratory setting, at reduced expenditures in time and money.

There have been several studies of respiratory airflow dynamics in the past few years. The structure of human bronchial airways can be approximated as a network of repeatedly bifurcating tubes. The symmetric Weibel configuration is most frequently employed because of its ease-of-use and common comparability. Schroter and Sudlow [2] made the earliest experimental study of airflow dynamics with a human respiratory network. The test model was at Reynolds numbers (based on local diameter) ranging from 50 to 4,500. They concluded that the inspiratory flows were independent of both Reynolds number and entry velocity profile. Other experimental studies [3-6] of the respiratory airflow dynamics further concluded that the respiratory flow patterns were likely dependent on the airway geometry. These studies concluded that quasi-steady conditions could be assumed for the respiratory flow. However, these investigations were based on the normal breathing condition with a simple symmetric bifurcation of the airway.

In additional to the above mentioned experimental works mentioned above, there also have been a number of studies using CFD in both two- and three-dimensional bifurcating tube models. Significant differences between the flow patterns predicted by the symmetric and asymmetric models and also between two- and three-dimensional models can be found. Gatlin et al. [8] found that the existence of separation regions occurring at the outer walls of the bifurcation (flow divider) in the two-dimensional models [7] was not apparent in the three-dimensional model. This was due to the three-dimensional effect or perhaps due to the sharp outer walls of the bifurcation suggested by Pedley [5]. Kurujareon et al. [9] investigated the effect of inlet boundary conditions on the numerical simulations of respiratory flow. The study used three-dimensional model of the central airway based on the anatomic details given by Horsfield et al. [10]. The simulation was generated using time dependent oscillatory flow for the normal breathing condition. The results showed the qualitative agreement of the flow features with the experimental works given by Menon et al. [11]. Although there are few studies using realistic models of the central airway, including asymmetric bifurcation and multiple generations of the branching [7, 8], the results are based on the assumption of the steady flow.

The aim of this study is to numerically simulate the time dependent flow phenomenon in a triple bifurcation airway model with its physiological inhalation mode for light activities.

ISSN: 1727-1983

Theory

The realistic tubular model representing the third to sixth generation human respiratory airways is shown in Fig. 1. The physiological inhalation mode for light activities [12] is shown in Fig. 2. An intermittent zero-flow period is used between two inspiratory cycles to replace the expiratory phase, because the experimental data have been obtained for inspiratory flow conditions only. The conduit is planar, smooth and rigid. The geometric data set for this system are summarized in Table 1-3. The complete breathing cycle and particle deposition will be considered in the future work.

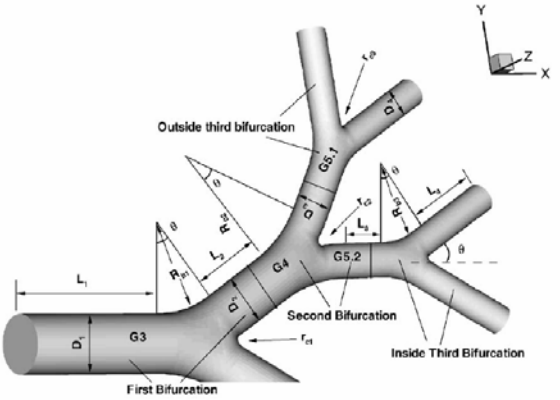

Figure1: Schematics of symmetric triple bifurcation geometry.

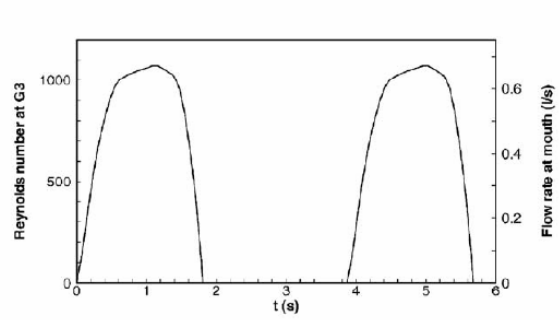

Figure 2: A typical inhalation waveform for normal light activity breathing.

Table 1: Geometric parameters for first bifurcation

Parent duct diameter	D_1	0.6
Daughter duct diameter	D_2	0.5
Length of ducts	L_1	2.4
	L_2	0.836
Bifurcation radius of curvature	R_{b1}	$2.7\,D_2$
Carinal radius of curvature	r_{c1}	$0.1\,D_2$
Bifurcation half-angle	θ	30°

Table 2: Geometric parameters for second bifurcation

Parent duct diameter	D_2	0.5
Daughter duct diameter	D_3	0.35
Length of ducts	L_3	0.437
Bifurcation radius of curvature	R_{b2}	$4.7\,D_3$
Carinal radius of curvature	r_{c2}	$0.1\,D_3$
Bifurcation half-angle	θ	30°

Table 3: Geometric parameters for third bifurcation

Parent duct diameter	D_3	0.35
Daughter duct diameter	D_4	0.29
Length of ducts	L_4	0.928
Bifurcation radius of curvature	R_{b3}	$2.7\,D_4$
Carinal radius of curvature	r_{c3}	$0.1\,D_4$
Bifurcation half-angle	θ	30°

For transient laminar incompressible flow, the fluid transport equations can be written as:

(Continuity)

$$\nabla \cdot \vec{v} = 0, \qquad (1)$$

(Momentum)

$$\rho \frac{D\vec{v}}{Dt} = -\nabla p + \mu \nabla^2 \vec{v} \qquad (2)$$

where p and $\vec{v}$ are the pressure fields and the velocity fields. The fluid is air with viscosity $\mu = 1.785 \times 10^{-5} kgm^{-1}s^{-1}$ and density $\rho = 1.18 kgm^{-3}$. Non-slip boundary conditions were imposed on the tube walls. The inlet velocity profiles were determined by the analytic expression of transient developed flow. The uniform pressure applied at the outlets is assumed, and its magnitude is preset the same as the reference pressure.

ICEM-CFD [13] was chosen as the pre-processing tool to generate the mesh based on the surface information obtained from the CAD models. Utilizing the assumed symmetry condition about the bifurcation plane, the flow field simulation involved only the upper half of the bifurcation model. Figure 3 shows the mesh topology for the bifurcated sections of airway model which was determined by refining the mesh until grid independence of the flow field solution was achieved. The final mesh of the triple configuration contained about 403,508 finite volumes. The numerical solution of the fluid flow equations (Eqs. (1) and (2)) were carried

ISSN: 1727-1983

out by employing a commercial finite-volume based program CFD-ACE [14]. The computations were performed on an SGI Origin 3800 computer with 48 GB of RAM and multiple 48 ×400 MHz CPUs. A fixed time step ($\Delta t = 0.02\,\mathrm{s}$) was used to calculate flow fields. A typical computing time required for simulation of each inhalation cycle was approximately 75 hours.

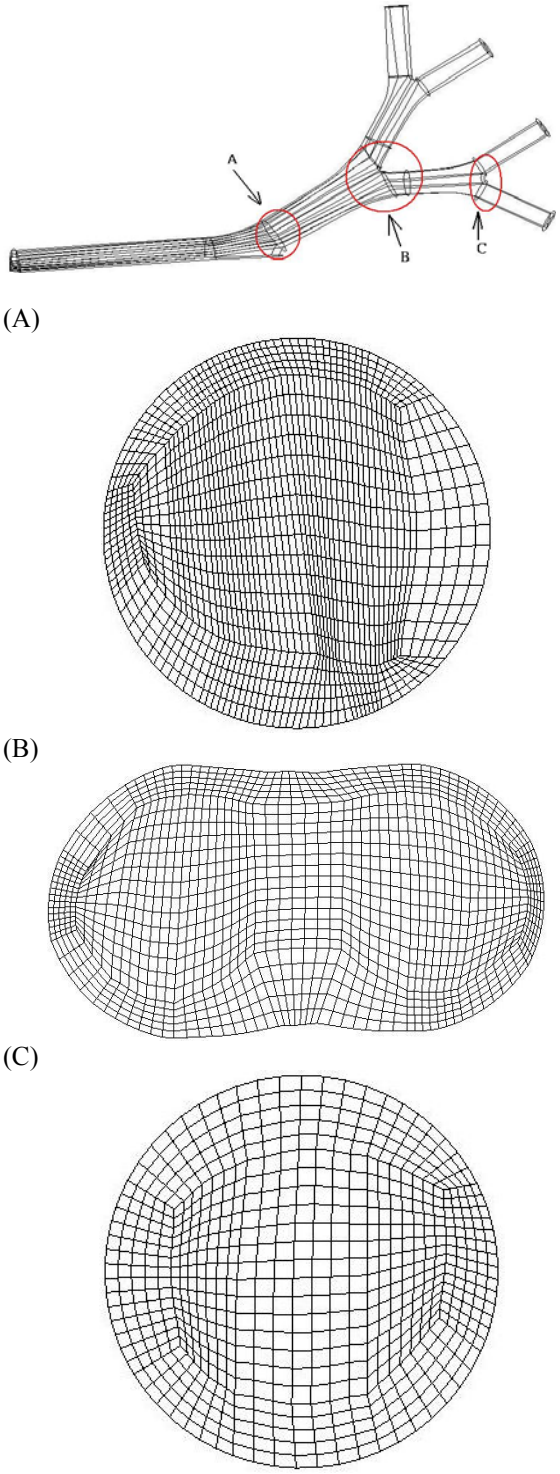

Figure 3: The mesh topology for the bifurcated sections of airway model.

Results and Discussion

The present simulation model has been validated with the computational fluid-particle dynamics model [15]. Typical air velocity field at two time levels (Re=805) during flow acceleration and deceleration are displayed in Figs. 4 and 5, respectively. The upper panel is a mid-plane view while the cross-sectional slices, A-A1, etc., show the secondary velocity contour. The distances between these cross sections and their corresponding upstream flow dividers are about 1.5 tube diameters.

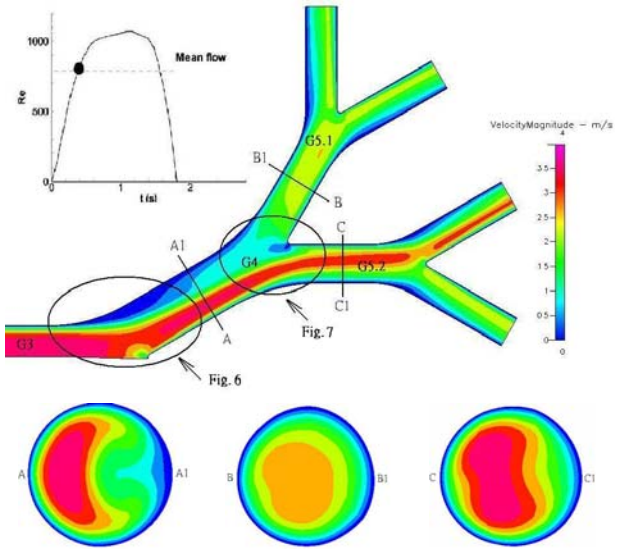

Figure 4: The mid-plane velocity contour profiles and selected cross-sectional secondary contour plot during flow acceleration.

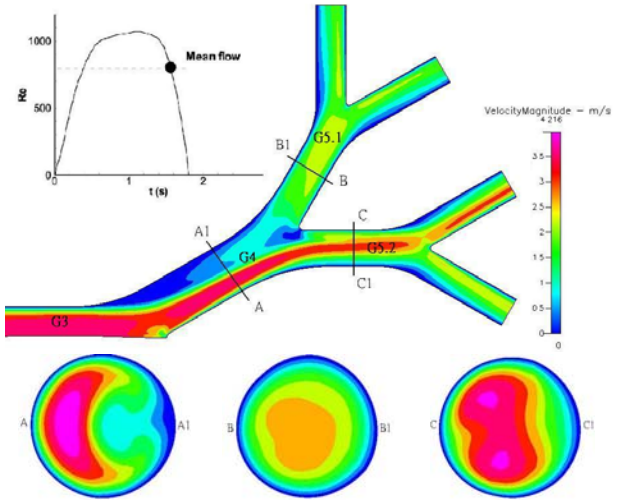

Figure 5: the mid-plane velocity contour profiles and selected cross-sectional secondary contour plot during flow deceleration.

ISSN: 1727-1983

The Flow Field during Flow Acceleration

The mid-plane velocity contour profiles along with some selected cross-sectional contour plots during flow acceleration are shown as in Fig. 4. The air stream splits at the first flow divider and a new boundary layer is generated at the inner wall of the first daughter tube (G4), where the maximum axial velocity stays near the inner wall. Subsequently, the interior of the second daughter tube (i.e., G5.2) experiences a higher air flow rate, and both the outside and inside third bifurcations encounter more uniform axial velocity profiles than the second bifurcations. The distinct shear layer along the inside wall after the first divider is thin, and a low flow region and even a recirculation zone are generated at the outer wall. Such a flow separation phenomenon as shown in Fig. 6 is related to the geometric features and the local Reynolds number. Generally speaking, if the local Reynolds number is high enough and the overall cross-sectional area is greater at downstream than upstream, there is a possibility of flow separation at the outer wall unless the geometry changes very smoothly. The ratio of the overall cross-sectional area of two first daughter tubes to that of the parent tube is 1:0.72 for the present geometry. The flow separation is generated slightly as shown in Fig. 7 at the second and third bifurcation because of the nearly constant cross-sectional area at the second bifurcation and the low local Reynolds number at the third bifurcation.

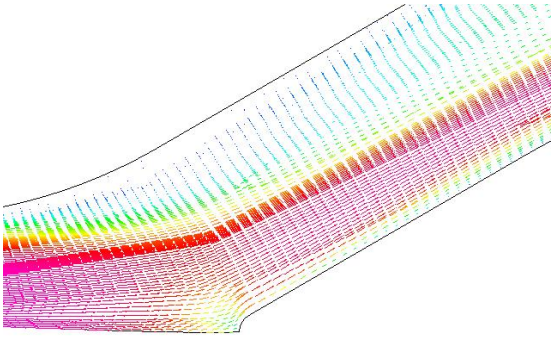

Figure 6: The velocity vectors at the first bifurcation.

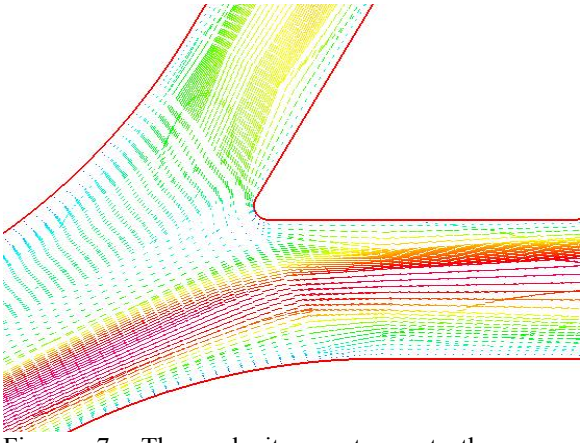

Figure 7: The velocity vectors at the second bifurcation.

Secondary Flow Generation

After the first flow divider, the air streams are deflected and secondary motions are generated. These vortices are formed because of the centrifugally induced pressure gradient in the normal direction which drives the slower moving fluid from the outside wall towards the inside wall, while the faster moving fluid around the top of the tube is swept outside. The secondary velocity field in cross section A-A1 exhibits one distinct vortex which moves the high-speed flow up around the top of the tube toward the outside of the bifurcation and low-speed flow from the outside of the bifurcation along the symmetry plane toward the inside of the bifurcation. The secondary motions in B-B1 and C-C1 are slightly different when compared to those in section A-A1 because of the geometric effects as well as the interaction between axial and secondary flows. Besides the vortex near the tube center, an additional co-rotating vortex rotates around the top to the outside wall in section B-B1or C-C1. The strength of secondary flow in section C-C1 located at G5.2, where the flow rate is higher, is much stronger than in section B-B1 located at G5.1.

The Flow Field during Flow Decelerating

Comparing the axial velocity contours in the decelerating phase of inspiratory f1ow (Fig. 5) with those during the accelerating phase (Fig. 4) at the same flow rate, we can observe some subtle differences because of the transient fluid inertia while the basic flow features remain the same. Both the magnitudes of axial and secondary velocities during flow deceleration are higher than those at acceleration for the same flow rate. This may be due to lingering effects of zero-flow before acceleration and peak-flow before deceleration. Generally, as the flow rate increases, the velocity profiles in the first daughter tube become more skewed due to boundary layer effects and convective acceleration, which result in an increasing flow asymmetry between the two subsequent daughter branches. The secondary flow effect in the daughter tubes also increases with the flow rate. The highest axial velocity in the inside second daughter tube rotates around the top and inside of the tube and lifts off from the symmetry plane during high flow rates.

Compared with Ref. [15], our result is similar to theirs. Our result shows that the maximum axial velocity stays near the outer wall (G5.2), but their result shows that the maximum axial velocity stays near the inner wall instead. The difference may be formed due to the particle iteration in the bifurcation airway model. Only flow field is simulated in our research.

Conclusions

This paper has addressed the flow field for a triple bifurcation lung airway model, representing Weibel generations G3-G6, under light activity breathing. The

ISSN: 1727-1983

air stream splits at the flow divider, and a new boundary layer may be generated depending on the ratio of the overall cross-sectional area of two first daughter tubes to that of the parent tube. Some subtle differences also can be observed by comparing the flow fields in the decelerating phase and accelerating phase of the inspiratory flow. The secondary motions were generated due to the complex geometry. With the CFD modelling, it is possible to develop an insight into airflow patterns and gain some valuable information.

In the future, our research team will use Magnetic Resonance Imaging (MRI) to generate a series of high-resolution 2D images. The profile of the trachea will be constructed by processing of these images. It follows with the creation of the geometry and meshes of the profile and then the aerosol transport and deposition phenomenon will be considered. The results may be used as a reference for the treatment of the respiratory diseases.

References

[1] Weibel, E. R. (1963): 'Morphometry of the human lung' New York, Academic Press.

[2] Schroter R. C., and Sudlow M. F. (1969): 'Flow patterns in model of the human bronchial airways', *Respir. Physiol.*, **7,** 341-355

[3] Chang H. K., and EI Masry OA. (1982): 'A model study of flow dynamics in human central airways. Part I: axial velocity profiles', *Respir. Physiol.*, **49**, 75-95

[4] Isabey D., and Chang H. k. (1982): 'A model study of flow dynamics in human central airways. Part II: secondary flow veclocities', *Respir. Physiol.*, **49**, 97-113

[5] Pedley T. J. (1977): 'Pulmonary fluid dynamics', *Ann. Rev. Fluid Mech.*, **9**, 229-274

[6] Zhao Y., and Lieber B. B. (1994): 'Steady expiratory flow in a model symmetric bifurcation', *ASME J. Biomech. Eng.*, **116**, 318-323

[7] Wilquem F., and Degrez G. (1997): 'Numerical three-generation model of the human central airways', *ASME J. Biomech. Eng.*, **119**, 59-65

[8] Gatlin B., Guicchi C., Hammersley J., Olson D. E., Reddy R., and Burnside G. (1995): 'Computational simulation of steady and oscillating flow in branching tubes', *ASME Bio-Medical. Fluids. Eng.*, **212**, 1-8

[9] Kurujareon J. (2000): 'Simulations of Airflow in the human tracheobronchial network', Ph.D. Thesis, University of Hertfordshire, UK

[10] Horsfield K., Dart G., Olson D. E., and Filley G. F. (1971): 'Models of the human bronchial tree', J. *Appl. Physiol.*, **31**, 207-217

[11] Menon A. S., Weber M. E., and Chang, H. K. (1984): 'A model study of flow dynamics in human central airways. Part III: oscillatory velocity profiles', *Respir. Physiol.*, **55**, 255-275

[12] Fenn W. O., and Rohn H. (1965): 'Handbook of physiology', Washington, DC: American Physiol. Society

[13] 'ANSYS ICEMCFD Documentation' , ANSYS, lnc

[14] 'CFD-ACE Documentation' , ESI-Group, lnc

[15] Zhang Z., Kleinstreuer C., and Kim C.S. (2002): 'Cyclic Micron-size Particle Inhalation and Deposition in a Triple Bifurcation Lung Airway Model', *Aerosol Science*, **33**, pp. 257-281

ISSN: 1727-1983